Water Vapor Flux-Profile Relationship in the Stable Boundary Layer over the Sea Surface

Yubin Ma[1], Xueling Cheng[2], Qilong Li[3], Lin Wu[2], Qingcun Zeng[2], Jiangbo Jin[2], ShiYong Shao[4], Junmin Li[5], and Chenghui Han[6]

[1]Institute of Atmospheric Physics Chinese Academy of Sciences
[2]Institute of Atmospheric Physics, Chinese Academy of Sciences
[3]Institute of Atmospheric Physics
[4]Anhui Institute of Optics and Fine Mechanics, Chinese Academy of Sciences
[5]South China Sea Institute of Oceanology, Chinese Academy of Sciences
[6]South Chin Sea Institute of Oceanology, Chinese Academy of Sciences

November 23, 2022

Abstract

Comprehensive marine atmospheric turbulence observation data, meteorological sounding and sea surface conditions in the South China Sea were employed to analyze and parameterize the vapor profile in the stable marine atmospheric boundary layer. The observations involved a three-dimensional ultrasonic anemometer, water vapor carbon dioxide analyzer, radiosonde and buoy. This paper theoretically determined that the water vapor profile function φ_χ differs from the temperature profile function φ_η and that φ_χ should be independently parameterized. A linear relationship existed between the dimensionless water vapor gradient and stability parameters based on the observation results, and φ_χ was then obtained as $\varphi_{\chi(\zeta/\Lambda)=\alpha(\zeta/\Lambda)+\beta}$, in which the stability covered the stability range (z/L>1). This result was applied in the Tropical Ocean-Global Atmosphere Coupled-Ocean Atmosphere Response Experiment (COARE) bulk flux algorithm, and the simulation of the latent heat flux was improved.

Hosted file

`essoar.10510923.1.docx` available at https://authorea.com/users/546101/articles/602274-water-vapor-flux-profile-relationship-in-the-stable-boundary-layer-over-the-sea-surface

Yubin Ma [1, 2] , † Xueling Cheng [1, 2] ,Qilong Li [1] , Lin Wu [1], † Qingcun Zeng [1], Jiangbo Jin [1] , Shiyong Shao [3] , Junmin Li [4] , Chenghui Han [4]

[1]Institute of Atmospheric Physics, Chinese Academy of Sciences, Beijing, China

[2]University of Chinese Academy of Sciences, Beijing, China

[3]Key Laboratory of Atmospheric Optics, Chinese Academy of Sciences, Hefei, China

[4]South Chin Sea Institute of Oceanology, Chinese Academy of Sciences, Guangzhou, China

Corresponding author:

Xueling Cheng (chengxl@mail.iap.ac.cn)

Qingcun Zeng(zqc@mail.iap.ac.cn)

Key Points:

- The linear relationship between the dimensionless specific humidity gradient and the stability parameter is established.
- The temperature mixing length is longer than the specific humidity ,and water vapor is more difficult to transfer in the vertical direction.
- In the model, the latent heat flux has better sensitivity to water vapor stability correction function.

Abstract

Comprehensive marine atmospheric turbulence observation data, meteorological sounding and sea surface conditions in the South China Sea were employed to analyze and parameterize the vapor profile in the stable marine atmospheric boundary layer. The observations involved a three-dimensional ultrasonic anemometer, water vapor carbon dioxide analyzer, radiosonde and buoy. This paper theoretically determined that the water vapor profile function differs from the temperature profile function and that should be independently parameterized. A linear relationship existed between the dimensionless water vapor gradient and stability parameters based on the observation results, and was then obtained as , in which the stability covered the stability range (). This result was applied in the Tropical Ocean-Global Atmosphere Coupled-Ocean Atmosphere Response Experiment (COARE) bulk flux algorithm, and the simulation of the latent heat flux was improved.

Keywords: Air-sea turbulent flux transport, Monin–Obukhov similarity theory, Stable boundary layer, Water vapor flux profile

Plain Language Summary

Monin and Obukhov established the relationship between momentum flux and temperature flux and their respective vertical gradients. Using these two relations and some parameterization methods, we can calculate momentum flux and

sensible heat flux. However, there is no physical basis for the above relationship for latent heat flux, and the effect of vertical distribution of water vapor on latent heat flux is not taken into account. In this paper, the relationship between water vapor flux and water vapor gradient is established and verified by marine observation data. Thus it can have more physical meaning and calculate the latent heat flux more accurately. This study is useful for understanding the boundary layer and model development.

1 Introduction

Understanding the characteristics of turbulent flux transport in the atmospheric boundary layer over the ocean is an important problem in the study of the atmospheric boundary layer. The importance of the turbulent flux between the ocean and atmosphere has been recognized in the development of earth system models, weather forecasts and environmental impact research. Our understanding of the behavior of turbulence in the atmospheric surface layer was vastly improved by a number of overland field experiments conducted in the late 1960s and 1970s. These experiments led to validation of the Monin–Obukhov similarity theory (MOST) (Monin and Obukhov, 1954), which is a modification of the logarithmic profile theory and establishes the relationship among the flux, meteorological element average profile and atmospheric stability. The theory has been verified, including the selection of the profile function form and determination of relevant parameters (Monin and Yaglom 1971; Dyer 1974; Yaglom 1977; Dyer and Bradley, 1982; Högström 1988; Sorbjan 1989; Garratt 1992; Andreas 2002; Grachev 2000; Grachev 2007). These relationships have often been applied to estimate the desired turbulent quantities from mean measurements over the ocean, where direct flux measurement is very difficult. However, the application of overland measurements to infer surface fluxes over the open ocean raises questions about the universality of these relationships. Researchers have given more attention to the dimensionless momentum gradient function φ_m and dimensionless temperature gradient function φ_h. However, there are few studies on the dimensionless water vapor gradient function φ_q. In regard to the air-sea boundary layer, bulk parameterization has generally been considered, and the exchange coefficient is therefore particularly important. Scholars are more concerned regarding the direct parametrization of the exchange coefficient or the roughness. Moreover, the influence of the stability is still obtained via relationships determined in the land boundary layer. Studies on the momentum and sensible heat flux exchange coefficient are numerous and mature, while studies on the water vapor exchange coefficient remain lacking. Sensible and latent heat fluxes are essentially the transport of temperature and specific humidity. Traditionally, it is assumed that the correlation coefficient between temperature and specific humidity is 1 or -1, because they are transported by the same turbulence in the same air mass. In the atmospheric surface layer(ASL), the correlation between the temperature (T) and specific humidity (q) is not high. There are a series of experiments, simulations and theoretical studies that can prove this, both over land (Mahrt 1976; Coulman 1980; de Bruin et al. 1993; Katul et al. 2008; Bink and Meesters 1997; McNaughton and Brunet 2002)and water

(Phelps and Pond 1971; Coulman 1980; Sempreviva and Højstrup 1998; Sempreviva and Gryning 2000; Li et al. 2012). However, until now, $\varphi_q(\xi) = \varphi_h(\xi)$ has generally been assumed, but the form of the water vapor stability correction function $\Psi_q(\xi)$ remains uncertain. This assumption has also been adopted in more advanced air-sea flux parameterization algorithms such as the Tropical Ocean-Global Atmosphere Coupled-Ocean Atmosphere Response Experiment (COARE) algorithm (Fairall, 1996). Today, the rapid development of earth system models globally, including the earth system model developed by the Institute of Atmospheric Physics (IAP), Chinese Academy of Sciences (CAS-ESM), further promotes the advancement of flux parameterization and generates unprecedented requirements for the flux calculation accuracy. Through calculation and simulation, momentum flux parameterization has been improved. However, the developed models still yield large errors in sensible and latent heat simulations. This has become a difficult problem for researchers worldwide. In terms of the COARE algorithm introduced by the CAS-ESM, the simulated global mean zonal wind stress is 0.0071 Pa, the observed global mean zonal wind stress is 0.0092 Pa, and the relative error thus reaches 22.8%. The simulated global mean latent heat flux is -94.53 W m^{-2}, while the observed value is -89.23 W m^{-2}, with a relative error of 5.9%. The simulated global average sensible heat flux is -14.69 W m^{-2}, and the corresponding observed value is -10.02 W m^{-2}, with a relative error of 46.6%. At present, effective methods are available for accurate water vapor measurement, which has provided us with a technical premise to study and describe the form of the water vapor profile more accurately. After research and discussion, we found that the assumption that the dimensionless water vapor gradient equals the dimensionless temperature gradient is inaccurate in practical applications, and enhancement of temperature and water vapor flux research could notably impact heat flux parameterization improvement.

2 Theory and Parameterization

The MOST (Monin and Obukhov, 1954) provides a framework to describe atmospheric turbulence in the surface layer. Monin and Obukhov proposed that in a nonuniform ASL with a given potential temperature, the influence of atmospheric stability or instability is limited, and turbulence is only determined by dynamic factors. Therefore, the height of the sublayer of dynamic turbulence (with a length scale) was given, which was subsequently referred to as the Obukhov length.

,

where is the friction velocity, is the virtual potential temperature, is the von Kármán constant (generally 0.4), g is the gravitational acceleration, and is the virtual potential temperature flux. For convenience, scholars have usually considered the height and Obukhov length jointly via the stability parameter , where is the height. In regard to the stability parameter , in which $z > 0$ in the atmospheric boundary layer above the sea surface, the sign mainly depends on the sign of the Obukhov length L. The influence of water vapor on stability

over the sea surface cannot be ignored, and the marine Obukhov length can be defined as follows:

,

where:

.

, and are the momentum, temperature and specific humidity fluxes, respectively. These three fluxes can be observed through high-frequency observation of the corresponding time via the eddy correlation method. In Eq. (2), and are constants greater than 0. At low latitudes (30°N~30°S), is generally greater than zero. Ignoring the influence of the specific humidity flux, the sign of L mainly depends on the sign of the momentum and temperature fluxes. When the transport directions of the momentum and temperature fluxes coincide, these fluxes remain stable at . When the transport directions of the momentum and temperature fluxes are opposite, or applies, and instability could occur at . Furthermore, the flux is transported along the gradient , and , where is the turbulent momentum exchange coefficient, and is the turbulent heat exchange coefficient. In addition, , with . Generally, the wind speed increases with the height, i.e., . The sign of the stability largely depends on the change in the potential temperature with the height . This is consistent with the Richardson number criterion.

The dimensionless turbulent velocity gradient is generally assumed as a function of the stability parameter :

.

The dimensionless turbulent potential temperature gradient is commonly assumed as a function of the stability parameter:

.

This paper focuses on the water vapor flux and vertical distribution of water vapor variables. We suppose that the dimensionless gradient of the specific humidity exhibits a similar relationship with (relevant proof is provided in Section 4):

.

Vertical integration of the dimensionless expansion equation yields the following:

,

where is the saturated vapor pressure at the air-sea interface, which is a function of the sea surface temperature, , and is the water vapor roughness similar to the momentum roughness. At the considered height, the specific humidity of air is the same as that at the sea surface, and the value is generally very low. However, due to the problem of calculation convergence, a value of 0 cannot be directly employed. According to previous studies, this value is generally set to or smaller (Andreas, 1987).

The water vapor stability correction function is:

.

Substitution of Eq. (9) into Eq. (8) generates the following:

.

Therefore, the specific humidity scale , specific humidity flux and latent heat flux can be parametrically calculated as:

.

where .

.

The calculation of the latent heat flux, i.e., Eq. , is based on the selection of a dimensionless water vapor gradient . In parameterization algorithms, such as the COARE algorithm, researchers have assumed that and are equal, which does not reflect the vertical distribution of water vapor in the boundary layer in detail.

In addition, physically, the Clausius–Clapeyron equation is:

,

where e_s is the saturated water vapor pressure, is the latent heat of vaporization, and is the moist air mole gas constant. Eq. (15) describes the variation in the saturated water vapor pressure across a flat surface with the temperature, and the temperature determines the maximum water vapor per unit air. However, it is unreasonable to assume that the profile shapes of these two quantities are always the same because we cannot require that saturated water vapor always occurs or that the relative humidity is always certain.

3 Data and Methods

The observation data considered in this paper originated from the South China Sea onboard observation experiments conducted by the Institute of Atmospheric Physics (IAP), Chinese Academy of Sciences and South China Sea Institute of Oceanology (SCSIO), Chinese Academy of Sciences, from September 2020 to November 2020. The ship Experiment One was equipped with an ultrasonic anemometer (100 Hz, UAT-3, IAP), a water vapor carbon dioxide analyzer (20 Hz, Li-7500A, LiCor Inc., Lincoln, Nebraska, USA), a combined navigator instrument (xw-GI5651,50hz), which could measure the attitude, azimuth and moving speed of the carrier in real time and could accordingly correct the measured meteorological and marine variables, and a sounding balloon equipped with a temperature pulsation device, water vapor instrument and barometer, which could measure vertical profiles of meteorological elements such as the temperature, humidity and air pressure at sea. In addition, the SCSIO released marine buoys to measure the sea surface temperature and shallow water velocity and flow direction during this period. Vertical profiles of the relative humidity,

temperature and wind speed were obtained. To acquire better statistics of vertical profile characteristics over sea, four radiosondes were deployed each day at 0000, 0600, 1200 and 1800 local time (LT) (LT = UTC + 8 h).

In this work, three-dimensional wind speed components u, v and w of the ultrasonic anemometer, carbon dioxide number concentration, water vapor number concentration, atmospheric pressure, atmospheric temperature, sea surface temperature measured by the buoy, flow velocities along the streamwise and cross-wind directions of the sea surface, and temperature and relative humidity profiles obtained by the radiosonde were mainly considered.

The obtained water vapor data included the relative humidity, which is the ratio of the mole fractions of water vapor and saturated water vapor at a certain temperature and pressure. It can be deduced that the relative humidity is the ratio of the water vapor pressure and saturated water vapor pressure at a certain temperature and pressure:

,

where RH is the relative humidity, e is the vapor pressure, is the saturated vapor pressure, T is the air temperature in K, and P is the air pressure. With the above equation, we can determine the water pressure as follows:

.

Suppose the mole fraction of water vapor in wet air is:

,

where is the mole fraction of water vapor, denotes the moles of water vapor, denotes the moles of dry air, is the water vapor mass, is the dry air mass, is the water vapor mole mass, and is the dry air mole mass. The mixing ratio is , and the ratio of the molar masses of water vapor and dry air is .

The vapor pressure is given as:

.

Thus, the mixing ratio is related to the water vapor pressure as follows:

.

The mass ratio of water vapor and wet air is defined by the specific humidity as:

.

Then, via replacement of the water vapor pressure, the observed relative humidity can be converted into the specific humidity. If the specific humidity is observed, no conversion is required.

The saturated water vapor pressure over the water surface or ice surface can be obtained with the following empirical equation (WMO, 1988), where t is expressed in °C.

.

In regard to wet air, the following air pressure correction is applied:

.

Considering a sea surface with a salinity of 34 ‰, should be multiplied by 0.98 (Sverdrup, 1942).

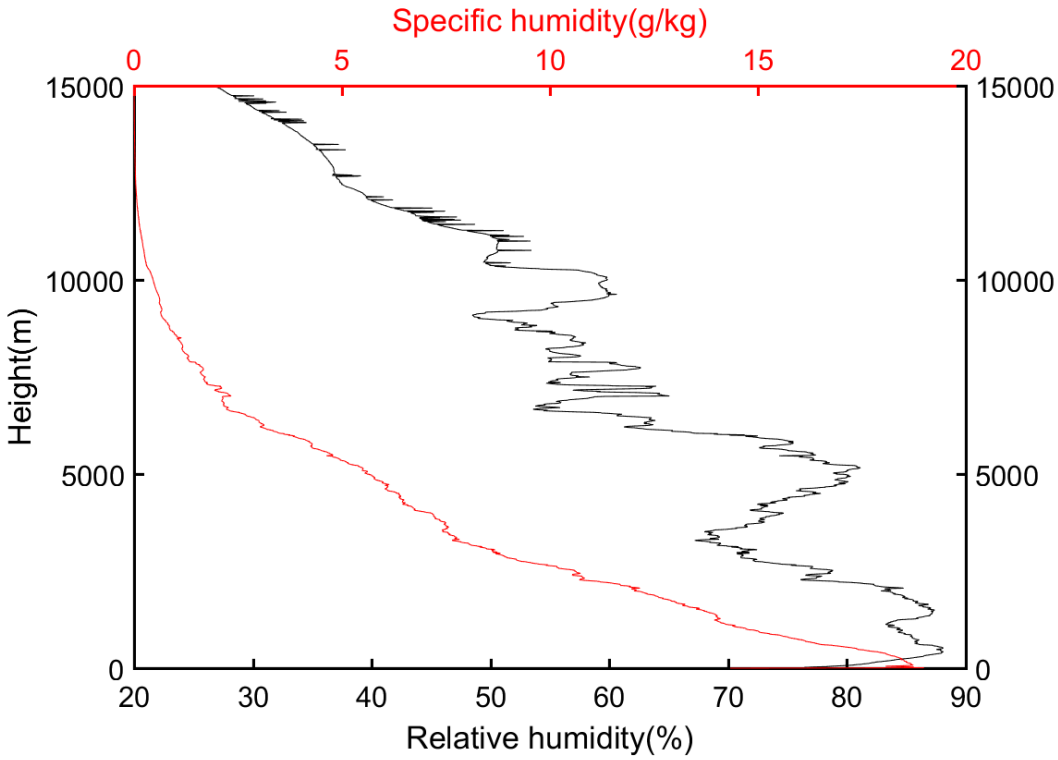

Fig. 1 Relative and specific humidity with the height. The black and red lines indicate the relative and specific humidity, respectively.

As shown in Fig. 1, the relative humidity was derived as the average radiosonde-measured value, and the specific humidity was calculated with Eq.. The consistency in the specific humidity was greater than that in the relative humidity. The upper abscissa indicates the specific humidity in g kg^{-1}, the lower abscissa indicates the relative humidity in %, and the ordinate indicates the height. With decreasing temperature, the maximum water vapor per unit air decreased, and the specific humidity thus continuously decreased. Moreover, the monotonicity of the specific humidity was more notable than that of the relative humidity. Hence, it is easier to establish physical laws based on the specific humidity.

4 Results and Discussion

4.1 Water vapor flux-profile relationship

First, we explain why the assumption of is unreasonable. According to the constant flux approximation in the surface layer, the specific humidity, momentum and heat fluxes do not vary with the height and are only functions of and . As expressed in Eq. (2), does not change with the height, but the specific humidity and temperature gradients vary with the height, and the gradients differ between the various heights. Hence, we obtain the following:

.

According to the observation data, we can directly calculate , as shown in Fig. 2.

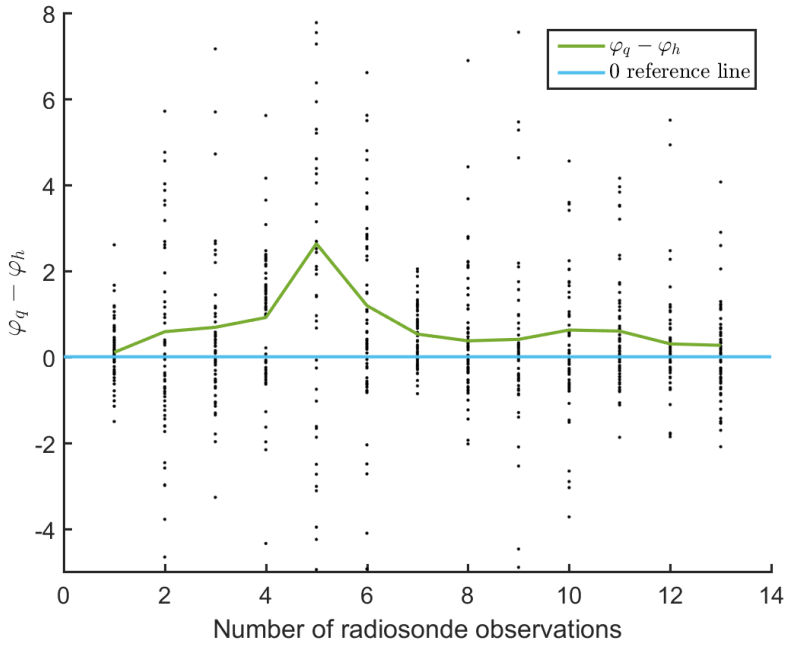

Fig. 2 Difference between the dimensionless water vapor gradient and dimensionless temperature gradient. The scatter points indicate at the different heights, the green line indicates the average gradient difference in the boundary layer, and the blue line is the 0 reference line.

As shown in Fig. 2, the abscissa indicates the number of observations, the ordinate indicates the difference between the dimensionless specific humidity and temperature gradients, and the green line indicates the average difference with the height. The blue line is the 0 reference line. Through analysis of the overall actual observation conditions, the values are not equal to 0, i.e., .

In addition, in regard to the height average, the dimensionless specific humidity gradient is always higher than that of the temperature.

According to the Prandtl mixing-length theory, the following applies:

,

.

The above can be obtained by substituting Eqs. and into Eq. . The above includes the turbulent specific humidity exchange coefficient and turbulent heat exchange coefficient:

.

Based on the observation results, we can obtain the following:

.

Because is positive, we can obtain:

.

The flow heat exchange coefficient is higher than the turbulent specific humidity exchange coefficient. Furthermore, , where V is the turbulent velocity scale and is the mixing length. Similar to the momentum mixing length, we defined the temperature mixing length and water vapor mixing length , where is an artificially assumed distance within which the eddy temperature remains constant. However, beyond , the eddy temperature completely blends with that of the surrounding fluid. The vapor mixing length can also be defined in a similar manner, as follows:

.

Since the turbulent motion velocity scale of the heat and water vapor transportation process is the same, the following applies:

.

In regard to the mixing layer, the following can be deduced:

.

The temperature mixing length is larger than the water vapor mixing length. Turbulent eddies carry heat and water vapor simultaneously. As the temperature mixing length is longer, the temperature attribute of turbulent eddies does not vary across a large distance, while the water vapor attribute of turbulent eddies can only remain unchanged across a short distance. Hence, water vapor is more difficult to transport than is heat along the vertical direction.

There is also a simple physical explanation. First, the water vapor pressure per unit of air depends on the temperature, and at a low temperature, only a small amount of water vapor can be retained. To transport more water vapor, a higher air temperature is required. Second, water vapor phase transition occurs

during the rising process of air parcels, and further water vapor condensation can release latent heat, thus inhibiting temperature reduction. In particular, phase transition during air parcel rise is beneficial for heat transfer but not for water vapor transfer.

4.2 Dimensionless specific humidity gradient in linear form

As supposed in Section 2, the dimensionless specific humidity gradient function is:

,

can be calculated according to the vertical difference in the specific humidity, as converted in Section 4.1.

The relationship between the dimensionless specific humidity gradient and stability parameter is shown in Fig. 3.

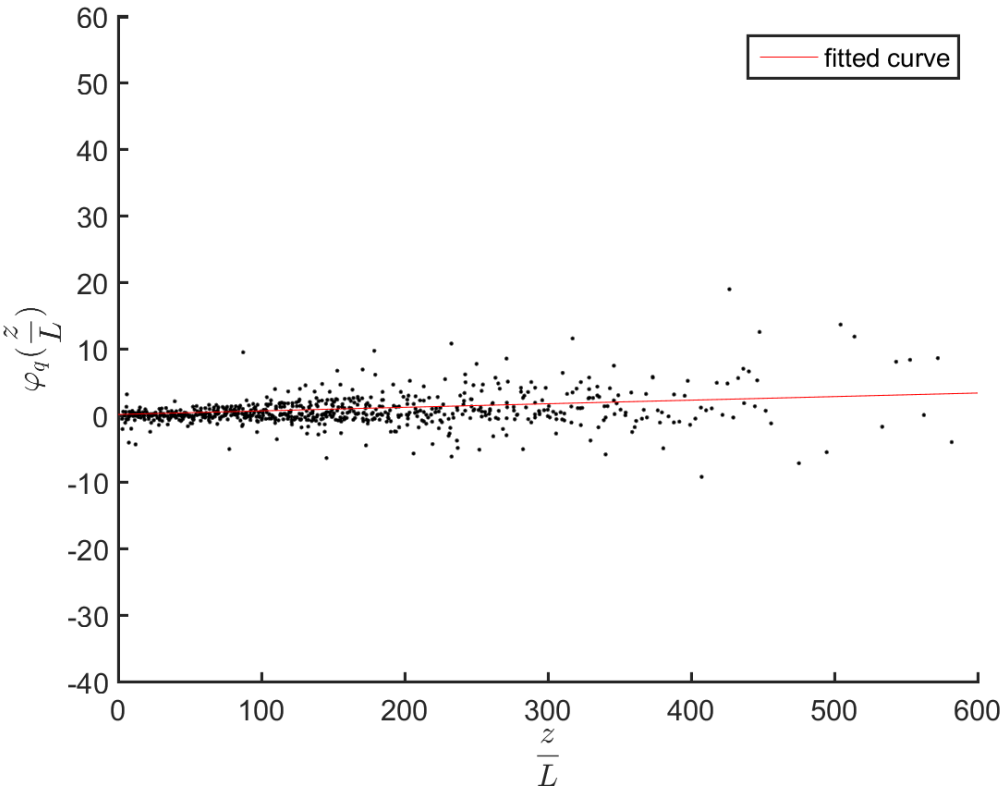

Fig. 3 Relationship between the dimensionless specific humidity gradient and stability parameters.

The ordinate indicates the dimensionless specific humidity gradient, and the

abscissa indicates the stability parameter. The scattered points indicate the dimensionless specific humidity gradient calculated based on the radiosonde and flux measurements in the boundary layer, and a good linear relationship can be observed. Therefore, the linear form of can be further assumed as:

.

Considering the continuity in the water vapor stability correction function under neutral conditions, b remains fixed as 1. The relationship could then be fitted with $a = 0.63$ and $b = 1$. The multiple correlation coefficient value reached 0.87, and the adjusted correlation coefficient value was 0.87. The multiple and adjusted correlation coefficient values approached 1, the sum of the squared error (SSE) reached 188.8, and the root mean square error (RMSE) was 1.6. The SSE and RMSE values were small, and the fitting result was satisfactory. Thus, the linear model suitably described the relationship between the specific humidity dimensionless gradient and. Furthermore, through substitution of the obtained linear form into Eq. (9), the specific humidity stability correction function is as follows:

.

Because the linear form was selected, integration of the water vapor stability correction function could be conveniently achieved, and the form was also very simple and practical. Regarding stability at sea, . In terms of instability at sea, the and forms remain unknown and should be further studied (the form should still be applied). A comparison of and is shown in Fig. 4.

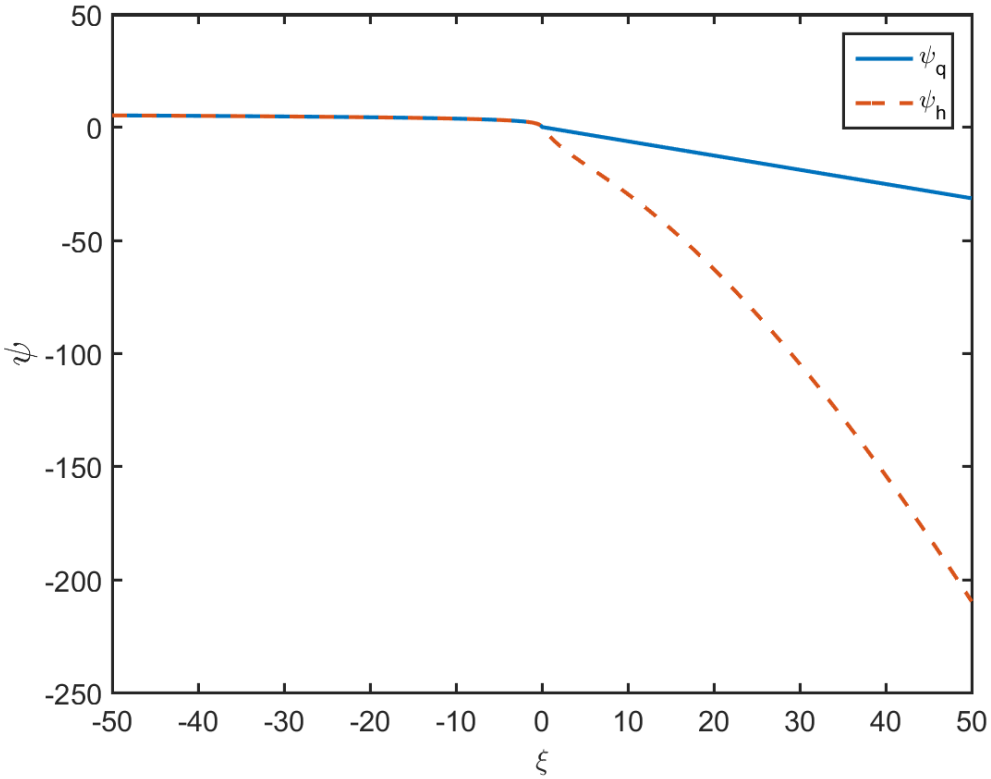

Fig. 4 Water vapor and temperature stability correction function comparison.

Through substitution of the obtained water vapor stability correction function (Eq.) into Eq. , the latent heat flux can thus be calculated. This scheme considers the relationship between the water vapor flux and profile and the vertical distribution of water vapor. Compared to the previous scheme, the physical significance is more obvious, and the latent heat exchange coefficient differs from the sensible heat exchange coefficient.

4.3 Application of the water vapor stability function to the flux algorithm

Stability parameters are described in Section 2. Above the ocean surface, these stability parameters are generally greater than zero, and the atmosphere occurs in a stable state most of the time. The condition of is rare. Therefore, we initially substituted the newly constructed stability correction function into the COARE flux algorithm instead of applying as , and the obtained results were compared.

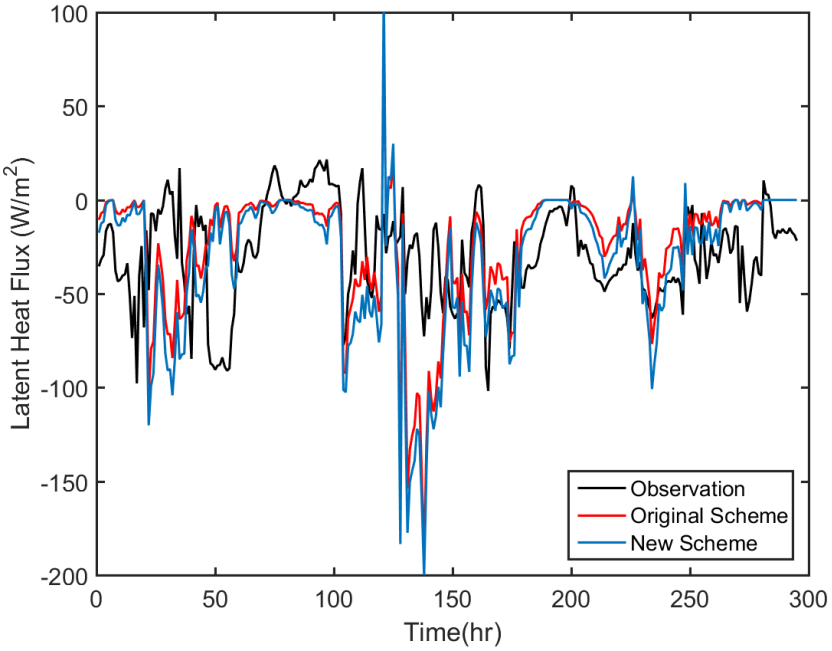

Fig. 5 Latent heat flux simulation sensitivity to the vapor stability correction function.

The latent heat simulated with the old and new schemes is shown in Fig. 5, in which the abscissa indicates the observation time, the total duration is 294 hours, and the ordinate indicates the latent heat flux value. The black line indicates the observations. The red solid line indicates the original results obtained under the hypothesis of . The blue line indicates the introduced latent heat flux . The sign reflects the direction of latent heat flux transfer. A minus sign indicates latent heat transport from the ocean to the atmosphere. Conversely, a plus sign indicates latent heat transfer from the atmosphere to the ocean.

As expected, the calculation of the latent heat flux was improved through the introduction of . Adopting the covariance flux calculation results as observations, the average observed latent heat flux reached -28.7, and the simulated latent heat flux in the form of was -24.3. Compared to the observed flux, the relative error reached 15.07%. The simulated latent heat flux in our proposed form of reached -32.4, and the relative error was 12.93%. The result obtained with the new scheme was closer to the observation, and the error was reduced by 0.6. It could be observed that the introduction of the independent form improved the simulation of the latent heat flux. Compared to the original scheme, the latent heat simulation value under the new scheme changed by 8, and the latent heat flux was sensitive to the water vapor stability correction function.

5 Conclusions

Most flux algorithms are based on the MOST, which only proposes relationships between the momentum and temperature fluxes and stability parameters. These two relationships have been verified by predecessors over the past decades, and many studies have been conducted regarding the selection of momentum and temperature dimensionless gradient functions. However, the profile relationship of the water vapor gradient considered in the calculation of the latent heat flux in these models does not provide a theoretical basis. The assumption that the water vapor and temperature gradients are equal is not accurate in actual calculations.

Through physical analysis, we proposed a profile relationship of the water vapor gradient. This observation could provide a basis for accurate measurement of the turbulent water vapor flux and profile in the boundary layer. Relevant flux-profile data were obtained from a comprehensive observation experiment in the South China Sea. First, we theoretically explained that the assumption of $\varphi_q(\xi) = \varphi_h(\xi)$ in parametric algorithms such as the COARE algorithm is unreasonable. Second, a linear relationship between the dimensionless water vapor gradient and stability parameters was established based on the obtained flux-profile data (the stability covered the relatively stable range). Integration was performed to obtain a water vapor stability correction function, which was subsequently applied in the COARE flux algorithm. Compared to the algorithm without a separate water vapor stability correction function, the new algorithm enhanced the simulation of the latent heat flux. In the future, we will continue to accurately measure and correct the relationship between the water vapor flux and profiles, which is very important to explain and simulate the processes of latent heat flux transfer and precipitation.

In addition, our vertical mean of $\varphi_q(\xi) - \varphi_h(\xi)$ calculated based on the observations was always greater than 0. Therefore, the turbulent exchange coefficient of the temperature should be greater than that of water vapor in the boundary layer. It was further deduced that the temperature mixing length is larger than the water vapor mixing length. This is very important to better understand the boundary layer energy exchange process and deserves further study.

Acknowledgements This work was supported by the National Science Foundation of China under Grants 41630530 and 42175103, the National Key Research and Development Plan from the Ministry of Science and Technology of China under Grant 2018YFC0213102, the Youth Innovation Promotion Association, Chinese Academy of Sciences (Grant No. 2019079) ,Strategic Priority Research Program of the Chinese Academy of Sciences (XDA13030304) and the National Key Scientific and Technological Infrastructure project "Earth System Science Numerical Simulator Facility" (Earth Lab).

References

Andreas EL (1987) ,A theory for the scalar roughness and the scalar transfer coefficients over snow and sea ice. *Boundary-Layer Meteorol,* 38(1-2): 159-184

Bink NJ, Meesters A (1997), Comment on estimating surface heat and momentum fluxes using flux-variance method above uniform and non-uniform terrain. *Boundary-Layer Meteorol*, 84:497–502

Coulman C (1980), Correlation between velocity, temperature and humidity fluctuations in the air above land and ocean. *Boundary-Layer Meteorol,* 19:403–420

de Bruin HA, Kohsiek W, der Hurk JV (1993), A verification of some methods to determine the fluxes of momentum, sensible heat and water vapour using standard deviation and structure parameter of a scalar meteorological quantities. *Boundary-Layer Meteorol*, 63:231–257

Dyer AJ (1974), A review of flux–profile relationships. *Boundary-Layer Meteorol*, 7:363–372

Dyer AJ, Bradley EF (1982), An alternative analysis of flux–gradient relationships at the 1976 ITCE. *Boundary-Layer Meteorol,* 22:3–19

Edson JB, Jampana V, Weller RA, Bigorre SP, Plueddemann AJ, Fairall CW, Miller SD, Mahrt L,Vickers D, Hersbach H (2013), On the Exchange of Momentum over the Open Ocean. *J Phys Oceanogr,* 43(8): 1589-1610

Fairall CW, Bradley EF, Rogers DP, Edson JB, Young GS (1996), Bulk parameterization of air-sea fluxes for Tropical Ocean-Global Atmosphere Coupled-Ocean Atmosphere Response Experiment. *J Geophys Res* ,101(C2):3747-3764

Fairall CW, Bradley EF, Hare JE, Grachev AA, Edson JB (2003), Bulk Parameterization of Air--Sea Fluxes: Updates and Verification for the COARE Algorithm. *J Clim,* 16: 571-591

Garratt JR (1992), The atmospheric boundary layer. Cambridge University Press, Cambridge, 316 pp

Grachev AA, Andreas EL, Fairall CW, Guest PS, and Persson POG (2007), SHEBA flux-profile relationships in the stable atmospheric boundary layer. *Boundary-Layer Meteorol,* 124: 315-333

Grachev AA, Fairall CW, Bradley EF (2000), Convective Profile Constants Revisited. *Boundary-Layer Meteorol*, 94: 495-515

Högström U (1988), Non-dimensional wind and temperature profiles in the atmospheric surface layer: A re-evaluation. *Boundary-Layer Meteorol*, 42:55-78

Johansson C, Smedman AS, Hogstrom U, Brasseur JG (2002), Comments on "Critical test of the validity of Monin-Obukhov similarity during convective conditions" – Reply. *J Atmos Sci*, 59: 2608-2614

Katul GG, Sempreviva AM, Cava D (2008), The temperature–humidity covariance in the marine surface layer: a one-dimensional analytical model. *Boundary-Layer Meteorol*, 126:263–278

Li D, Bou-Zeid E, de Bruin HAR (2012), Monin-Obukhov similarity functions for the structure parameters of temperature and humidity. *Boundary-Layer Meteorol,* 145:45–67

Mahrt L (1976), Mixed layer moisture structure. *Mon Weather Rev*, 104:1403–1407

McNaughton KG, BrunetY(2002), Townsend's hypothesis, coherent structures and Monin-Obukhov similarity. *Boundary-Layer Meteorol,* 102:161–175

Monin AS, Obukhov AM (1954), Basic laws of turbulent mixing in the surface layer of the atmosphere. *Trudy Geofiz Inst Acad Nauk SSSR,* 24:163-187

Monin AS, Yaglom AM (1971), Statistical fluid mechanics: mechanics of turbulence, vol 1. MIT Press, Cambridge, Massachusetts, 769 pp

Phelps G, Pond S (1971), Spectra of temperature and humidity fluctuations and of fluxes of moisture and sensible heat in marine boundary layer. *J Atmos Sci,* 28:918–928

Sempreviva AM, Gryning SE (2000), Mixing height over water and its role on the correlation between temperature and humidity fluctuations in the unstable surface layer. *Boundary-Layer Meteorol,* 97:273–291

Sempreviva AM, Højstrup J (1998), Transport of temperature and humidity variance and covariance in the marine surface layer. *Boundary-Layer Meteorol,* 87:233–253

Sorbjan Z (1989), Structure of the Atmospheric Boundary Layer. Prentice-Hall, New Jersey, 317 pp

Yaglom AM (1977), Comments on wind and temperature flux-profile relationships. *Boundary-Layer Meteorol*, 11: 89-102